Reactions ^{58}Ni(^{3}He,^{3}He′) and ^{58}Ni(^{3}He,α) at 51.3 MeV*

C. R. BINGHAM† AND M. L. HALBERT
Oak Ridge National Laboratory, Oak Ridge, Tennessee 37830
(Received 25 October 1967)

Differential cross sections were measured for elastic and inelastic scattering of 51.3-MeV ^{3}He from ^{58}Ni, and for ^{58}Ni(^{3}He,α). The elastic scattering was analyzed in terms of the optical model with a Woods-Saxon potential. Several satisfactory sets of parameters were obtained. The inclusion of a spin-orbit term with $V_s \simeq 2.9$ MeV improved the best fits. The inelastic scattering events were treated as one-phonon collective transitions in the distorted-wave approximation, using complex coupling. The $\beta R_0'$ agreed well with deformation lengths from other experiments. No improvement in the fit to the 2^+ angular distribution was found in calculations with unequal real and imaginary deformations. The (^{3}He,α) results were compared with zero-range distorted-wave predictions, using a previously obtained empirical normalization. The spectroscopic factors are in good agreement with other experiments and sum-rule expectations.

I. INTRODUCTION

DISTORTED-WAVE analyses of inelastic scattering of ^{3}He to collective excited states seem to require a complex interaction.[1,2] In this type of calculation it is usually assumed that the spherical optical-model potential is deformed in an inelastic scattering event and that the deformation parameter is the same for both real and imaginary parts. For ^{3}He, the real part of the potential has a smaller radius than the imaginary part. It is possible that the deformations of the two are also different. This possibility was investigated during the analysis of the experimental data presented here. A detailed analysis of the elastic scattering is also given.

The (^{3}He,α) and (α,^{3}He) reactions in the Zr isotopes have been shown[2,3] to favor orbital angular momentum transfers of $l=5$ or 6 because the large Q value leads to quite different energies in the entrance and exit channels. Work on the ^{58}Ni(^{3}He,α) reaction has been reported at bombarding energies of 24.5 MeV,[4] and also at 15 and 18 MeV.[5] The (p,d) reaction favors smaller l transfers; hence, the (^{3}He,α) reaction supplements information obtained from (p,d) reactions. The ^{58}Ni(p,d) reaction has been studied at 18.5 MeV [6] and at 28 MeV.[7] These results will be compared with those from the present experiment on ^{58}Ni(^{3}He,α) at 51.3 MeV.

II. EXPERIMENTAL METHOD AND RESULTS

The experimental arrangement was described in detail previously.[2,3] The measurements were performed in the 30-in.-diam scattering chamber. Particles were detected in a counter telescope composed of a 500-μ surface-barrier detector and a 3-mm Li-drifted silicon detector operated at room temperature. Complete separation of the α and ^{3}He particles was achieved by registering the signal from the transmission counter versus the sum of the two signals in a 20 000-channel, two-parameter analyzer.

The target, placed at the center of the scattering chamber, was a 99.95% enriched ^{58}Ni foil 7.06 mg/cm^2 thick (obtained from the Isotope Target Center, Oak Ridge National Laboratory). Its thickness was determined by combining the measured energy loss of ^{241}Am α particles with range-energy data for nickel.[8] The energy-loss measurements showed that the foil is uniform within 6%. The uncertainty in target thickness causes the main error in the absolute cross sections, namely $\pm 10\%$.

The over-all energy resolution was about 190 keV. The straggling in the target accounts for about 110 keV. From the geometry of the analyzing magnet, the beam resolution was calculated to be 105 keV. The detectors probably account for the remainder of the observed energy spread.

Examples of ^{3}He and α-particle spectra are shown in Fig. 1. Data were obtained at 1° intervals from 9° to 74° (lab). The labeled peaks identify the groups that were studied systematically. The unlabeled peaks correspond either to scattering from impurities or to weak transitions in ^{58}Ni. The excitation energies in ^{58}Ni were calculated on the assumption that the energy of the first excited state is 1.452 MeV.[9] The energy scale for the α-particle spectra was determined from the ground state and the 5.22-MeV state observed in the ^{58}Ni(p,d) reaction.[5] Angular distributions derived for the labeled peaks of Fig. 1 are shown by the points in Figs. 2–4; the curves will be discussed below. The inelastic data at angles less than 25° are somewhat uncertain because of background coming from the huge elastic peak. For the weak transitions to states at

* Research sponsored by the U. S. Atomic Energy Commission under contract with Union Carbide Corporation.
† Present address: University of Tennessee, Knoxville, Tenn. 37916.
[1] E. R. Flynn and R. H. Bassel, Phys. Rev. Letters **15**, 168 (1965).
[2] C. R. Bingham and M. L. Halbert, Phys. Rev. **158**, 1085 (1967).
[3] C. R. Bingham, M. L. Halbert, and R. H. Bassel, Phys. Rev. **148**, 1174 (1966).
[4] D. E. Rundquist, Ph.D. thesis, University of Illinois (unpublished); M. K. Brussel, D. E. Rundquist, and A. I. Yavin, Phys. Rev. **140**, B838 (1965).
[5] Cheng-Ming Fou and Robert W. Zurmühle, Phys. Rev. **140**, B1283 (1965).
[6] J. C. Legg and E. Rost, Phys. Rev. **134**, B752 (1964).
[7] R. Sherr, B. F. Bayman, E. Rost, M. E. Rickey, and C. G. Hoot, Phys. Rev. **139**, B1272 (1965).
[8] L. C. Northcliffe, Natl. Acad. Sci.—Natl. Res. Council, Publ. No. 1133, 173 (1964).
[9] E. R. Cosman, C. H. Paris, A. Sperduto, and H. A. Enge, Phys. Rev. **142**, 673 (1966).

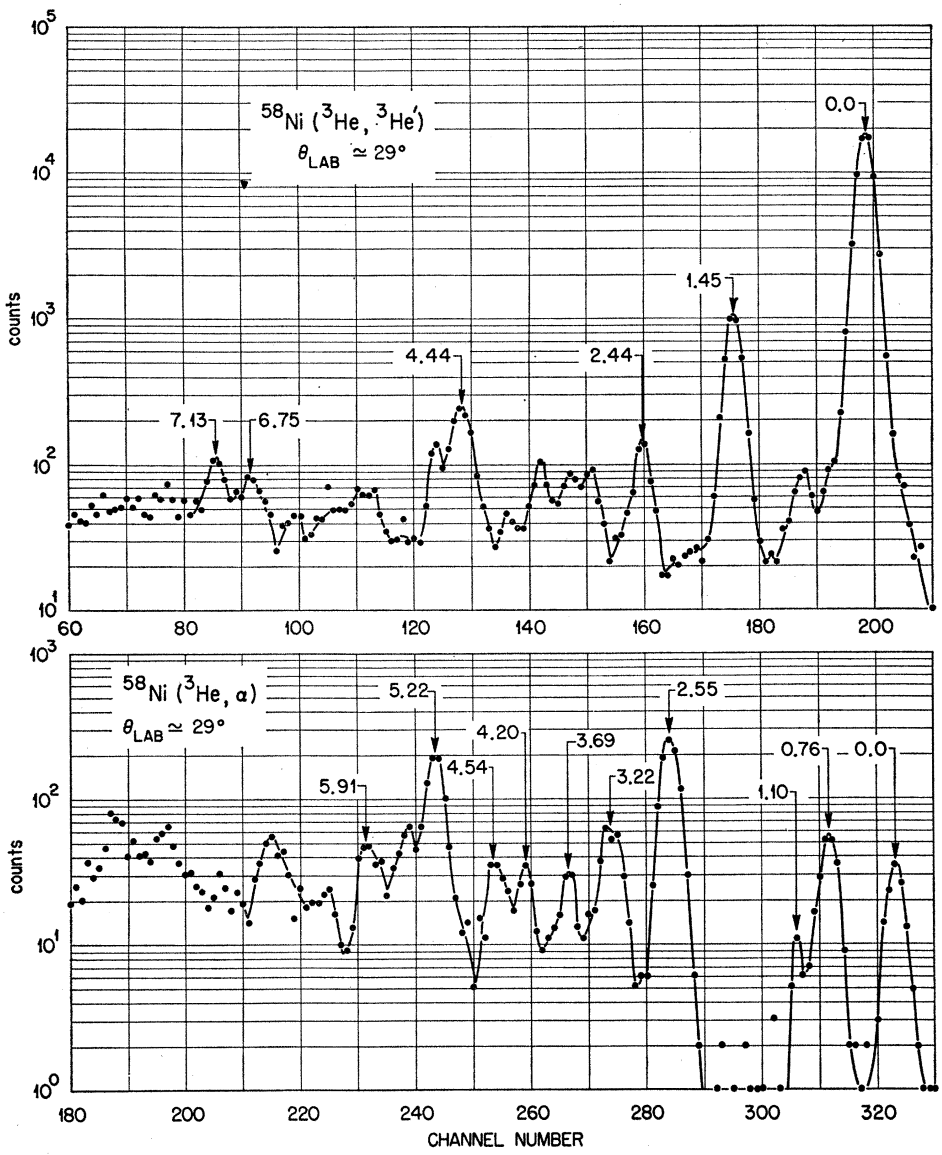

FIG. 1. Spectra of ^{3}He and α particles from ^{58}Ni bombarded with 51.3-MeV ^{3}He particles.

2.44, 6.75, and 7.13 MeV the problem exists at the larger angles also.

III. ELASTIC SCATTERING

The elastic scattering was analyzed in terms of the usual Woods-Saxon potential

$$V(r)=-\frac{V_0}{1+e^x}-\frac{iW_0}{1+e^{x'}}+\left(\frac{\hbar}{m_\pi c}\right)^2\frac{V_s\mathbf{L}\cdot\boldsymbol{\sigma}}{r(1+e^x)}+V_c,$$

where $x=(r-r_0A^{1/3})/a$, $x'=(r-r_0'A^{1/3})/a'$, and V_c is the Coulomb potential for a uniformly charged sphere of radius $1.4A^{1/3}$ F. The spin-orbit term was omitted from parts of the analysis. The free parameters V_0, r_0, a, W_0, r_0', a', and V_s were adjusted with an automatic search routine[10] to minimize the quantity

$$\chi^2=\sum_i\left(\frac{\sigma_{\rm th}{}^{(i)}-\sigma_{\rm expt}{}^{(i)}}{\Delta\sigma_{\rm expt}{}^{(i)}}\right)^2,$$

where $\sigma_{\rm th}{}^{(i)}$ and $\sigma_{\rm expt}{}^{(i)}$ are the calculated and experimental differential cross sections at angle θ_i, and $\Delta\sigma_{\rm expt}{}^{(i)}$, the weighting factor, is related to the estimated accuracy of $\sigma_{\rm expt}{}^{(i)}$. For the searches performed here, $\Delta\sigma_{\rm expt}{}^{(i)}$ was taken to be $\sim$6% of $\sigma_{\rm expt}{}^{(i)}$ for points below 55°, $\sim$12% of $\sigma_{\rm expt}{}^{(i)}$ for points between 55° and 72°; and $\sim$23% for points above 72°. Points in the sharp minimum were weighted somewhat less. In all cases, $\Delta\sigma_{\rm expt}{}^{(i)}$ was larger than the error due to counting statistics alone. The entire angular distribution was

[10] The HUNTER program, written by R. M. Drisko.

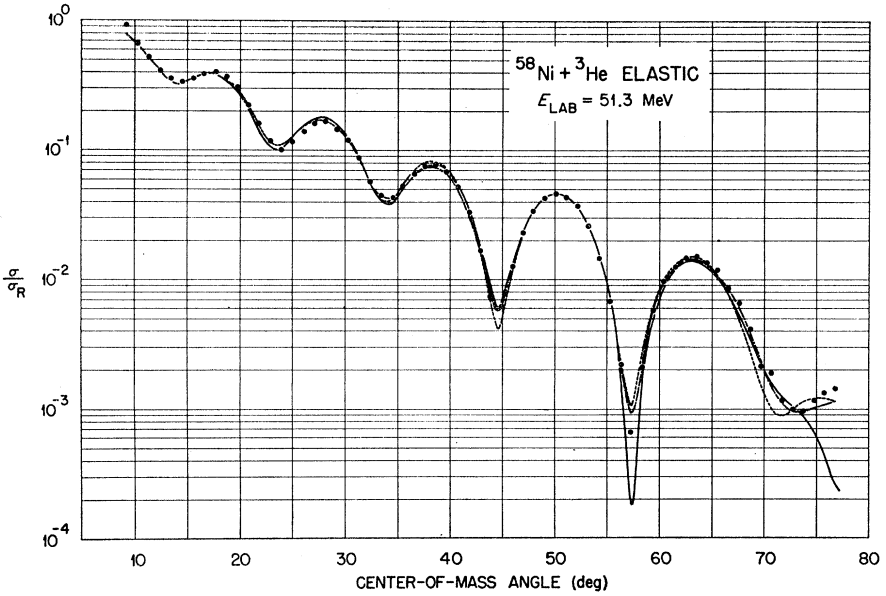

FIG. 2. Ratio of the elastic scattering cross section to the Rutherford cross section. The curves are least-squares fits with the potentials given in Table I: solid curve—*C*, dotted curve—*B*, dot-dash curve—*D*.

multiplied by a factor of 0.965 in order to improve the optical-model fits at small angles. This is well within the uncertainty in the target thickness. All reaction cross sections were normalized with the same factor.

The potentials shown in Table I were found to predict the ^{3}He scattering adequately. The fits obtained with potentials *B*, *C*, and *D* are shown in Fig. 2. Potential *A* was obtained by searching on V_0 and W_0 with the other parameters fixed to a standard geometry which works well for the elastic scattering of ^{3}He from various nuclei at lower energies.[11] The resulting V_0 and W_0 are very close to the values obtained with this geometry for many nuclei at energies from 20 to 51 MeV.[2,11] Potential *C* was obtained by searching on all the parameters starting with a potential similar to *A*. The real well depth increased substantially, and the geometry changed significantly, while χ^2 decreased by a factor of 2.3. This potential is similar to the one providing the best fit to the elastic scattering of 51.3-MeV ^{3}He by ^{92}Zr.[2] Potentials *E* and *G* are others having minima in χ^2, also found by searching on all parameters. Potentials *B*, *D*, *F*, and *H* were obtained by including the spin-orbit term in potentials *A*, *C*, *E*, and *G*, respectively, and performing searches again on the adjustable parameters. Except for the shallow potential (*G*), inclusion of the spin-orbit term decreased χ^2 significantly. This result contrasts with the finding that for ^{3}He on ^{92}Zr the spin-orbit term gives no improvement.[2] The improvement is restricted primarily to the largest angles. The spins of the protons in the ^{3}He are opposite and their spin-orbit effects tend to cancel. The orbital angular momentum of the neutron is approximately $\frac{1}{3}$ of that associated with the ^{3}He. Hence V_c for ^{3}He on ^{58}Ni is expected to be about $\frac{1}{3}$ of the single-nucleon value of about 6 MeV.[12] Thus, a spin-orbit well depth between 2 and 3 MeV is reasonable. The predicted polarizations (Basel convention) are shown in Fig. 5 for potentials *B* and *D*.

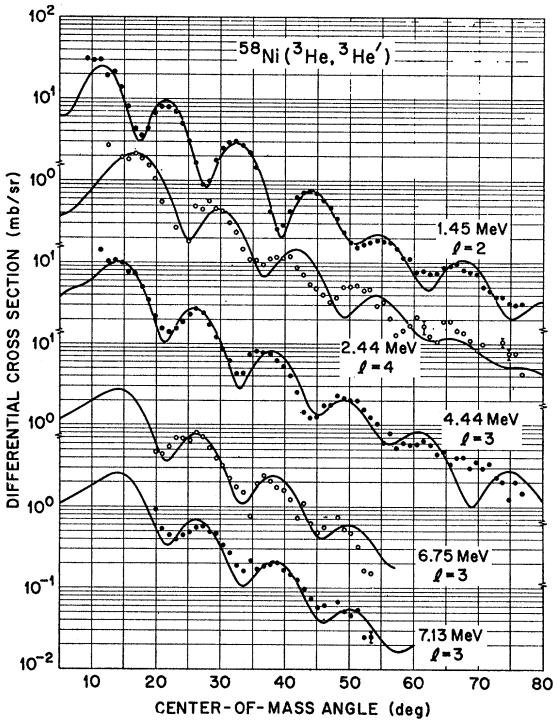

FIG. 3. Differential cross sections for inelastic scattering of 51.3-MeV ^{3}He by ^{58}Ni. The curves are distorted-wave predictions using potential *C*.

[11] R. H. Bassel (private communication); E. F. Gibson, B. W. Ridley, J. J. Kraushaar, M. E. Rickey, and R. H. Bassel, Phys. Rev. **155**, 1194 (1967).

[12] L. N. Blumberg, E. E. Gross, A. van der Woude, A. Zucker, and R. H. Bassel, Phys. Rev. **147**, 812 (1966).

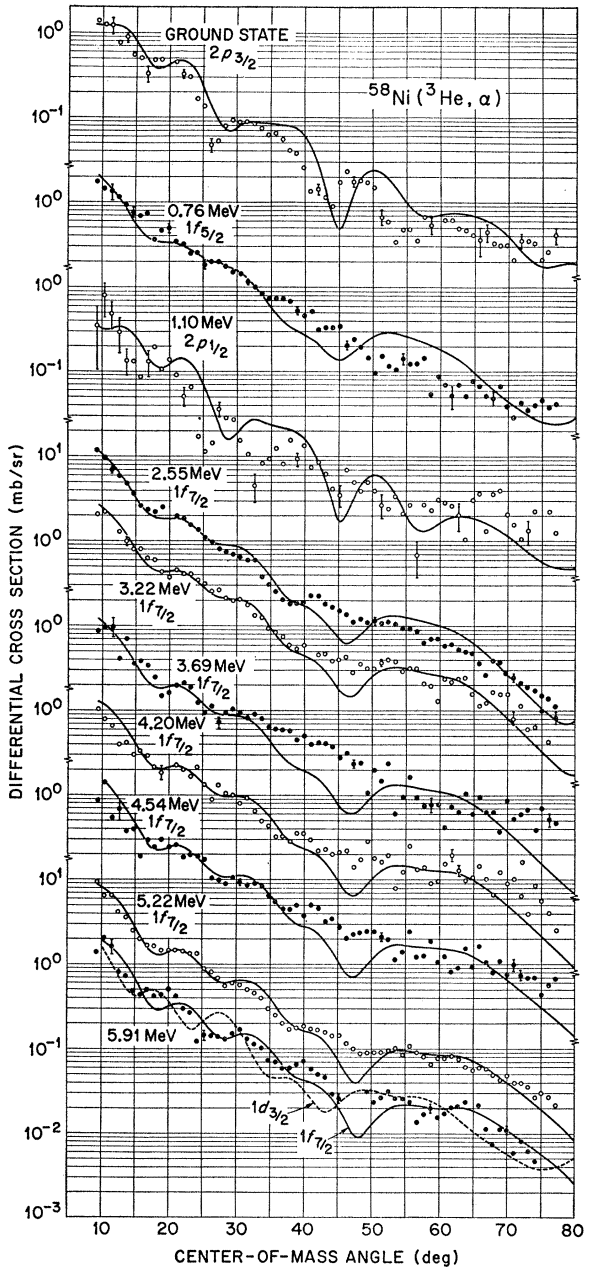

FIG. 4. Differential cross sections for ^{58}Ni(^{3}He,α) at 51.3 MeV. The curves are zero-range distorted-wave predictions.

IV. INELASTIC SCATTERING

The inelastic scattering was analyzed in terms of the collective model by means of the distorted-wave method.[13] A nonspherical optical potential was used. The spherical part describes the elastic scattering, and the nonspherical part is identified as the interaction responsible for the inelastic transition. Only one-phonon excitations were considered. In this model the transition amplitude has the form

$$T_{if}=\int d\mathbf{r}\,\chi_f^{(-)*}(\mathbf{k}_f,\mathbf{r}_f)\left\{i^l Y_l^m(\theta',\varphi')\left[\beta_R\frac{V_0R_0}{a}\times\frac{d}{dx}\left(\frac{1}{1+e^x}\right)+i\beta_I\frac{W_0R_0'}{a'}\frac{d}{dx'}\left(\frac{1}{1+e^{x'}}\right)\right]\chi_i^{(+)}(\mathbf{k}_i,\mathbf{r}_i)\right\},$$

where χ_i and χ_f are the distorted waves generated from the optical potentials for the initial and final states. Coulomb-excitation contributions were included for all transitions with angular momentum transfer $l<4$. The optical-model potentials measured for the entrance channel were also used for the exit channel. Potentials C and D predicted almost the same angular distributions and cross sections. Potential C was used for all the calculations presented here.

A number of calculations were made to investigate the interaction responsible for the inelastic scattering to the 2^+ state at 1.45 MeV. The deformation parameters β_R and β_I for the real and imaginary wells, respectively, were varied separately. Some of the results are compared with the experimental data in Fig. 6. The details of each calculation are given in Table II. The calculation with $\beta_I=0$ is out of phase at small angles and fits very badly at large angles, confirming earlier work with other nuclei, that a purely real interaction is inadequate.[1,2] The calculation using $\beta_R=0$ fits the data well at intermediate angles, but tends to oscillate too strongly at large angles. The somewhat better fit with $\beta_R=0$ than with $\beta_I=0$ illustrates the dominance of the imaginary part of the complex interaction.[2] The other three calculations, with $\beta_I=0.7\beta_R$, $\beta_I=\beta_R$, and $\beta_I=1.3\beta_R$ are almost equally good. There seems to be no justification here for using unequal real and imaginary deformations. The remainder of the results presented here are based on an interaction with one adjustable parameter, $\beta=\beta_R=\beta_I$. The magnitude of the predicted cross section is proportional to β^2.

The distorted-wave calculations for all the inelastic data are shown in Fig. 3. The deformation parameters are listed in Table III. The angular distributions predicted for the known 2^+ and 3^- levels at 1.45 and

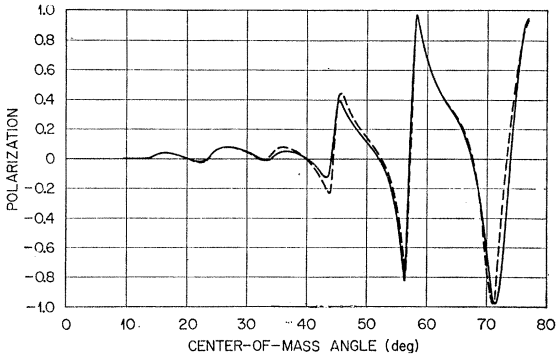

FIG. 5. Polarizations predicted by potentials D (solid curve) and B (dashed curve).

[13] The distorted-wave calculations were made with the program JULIE, written by R. M. Drisko.

TABLE I. Optical-model parameters for ^{58}Ni(^{3}He,^{3}He) at 51.3 MeV.

Potential	V_0 (MeV)	r_0 (F)	a (F)	W_0 (MeV)	r_0' (F)	a' (F)	V_s (MeV)	σ_R (mb)	χ^2
A	171.1	*1.14*[a]	*0.723*	16.99	*1.60*	*0.810*		1763	223
B	170.8	*1.14*	*0.723*	17.00	*1.60*	*0.810*	2.93	1763	93
C	209.1	0.992	0.828	16.58	1.66	0.700		1701	96
D	190.8	1.06	0.775	15.88	1.64	0.764	2.92	1746	32
E	143.2	1.02	0.881	14.69	1.71	0.662		1695	80
F	136.1	1.06	0.847	13.80	1.71	0.701	2.26	1724	43
G	88.1	1.06	0.981	13.32	1.75	0.624		1693	283
H	87.5	1.06	0.976	13.12	1.75	0.628	0.91	1697	282

[a] Italic parameters were held fixed.

TABLE II. Deformation parameters for calculations shown in Fig. 6.

β_I/β_R	β_R	β_I	$\beta_R R_0$	$\beta_I R_0'$
0	0.405	0	1.555	0
0.7	0.204	0.143	0.783	0.917
1.0	0.163	0.163	0.626	1.045
1.3	0.132	0.172	0.507	1.103
∞	0	0.216	0	1.385

4.44 MeV are in good agreement with the data. The 4^+ state at 2.44 MeV is part of a two-phonon triplet.[14] A coupled-channel calculation is needed to give a meaningful comparison with theory. Hence the curve shown in Fig. 3 for the 4^+ state only illustrates the inapplicability of the present theory and no deformation parameter is given for this state in Table III. The angular distributions for groups at 6.75 and 7.13 MeV are fitted quite well by $l=3$ predictions. The deformation lengths are compared with other results[15–18] in Table III. The agreement of $\beta R_0'$ with the deformation lengths from other experiments again demonstrates the dominance of the imaginary part of the interaction.

V. (^{3}He,α) REACTIONS

The (^{3}He,α) transitions to states in ^{57}Ni were analyzed with the zero-range distorted-wave theory with local potentials.[13] The bound-state wave function of the picked-up neutron was calculated for a Woods-Saxon potential with $r_0=1.2$ F and $a=0.7$ F. A spin-orbit term equal to 25 times the Thomas potential for nucleons was included. The depth of the central potential was adjusted to give an eigenvalue equal to the binding energy of the transferred neutron.

Potential *C* (Table I) was used to generate the entrance-channel distorted waves needed in these calculations. For the exit channel, which involves α particles between 54.7 and 61.1 MeV, optical potentials were obtained from the elastic scattering data of Darriulat *et al.*[19] for 64.3-MeV α particles on ^{58}Ni. Least-squares fits to their angular distribution were obtained with the four-parameter Woods-Saxon potentials given in Table IV. The Coulomb radius was held fixed at $1.4A^{1/3}$ F. The fit with potential *J* is shown in Fig. 7. Potential *K* gave an equally good fit.

Distorted-wave calculations were made for selected transitions using both potentials (*J* and *K*) for the exit channel with potential *C* for the entrance channel. The prediction using potential *J* fits the experimental angular distributions better. This confirms our earlier observations[2,3] that for a ^{3}He potential similar to potential *C*, an α-particle potential with $V_0\approx 100$ was the most satisfactory. It was for this reason that the shallow potential given in Ref. 19 was not used in our calculations. All further results presented here will use potentials *C* and *J*.

The initial and final configurations were assumed to be pure. The distorted-wave cross sections were calculated from

$$\frac{d\sigma}{d\Omega}=\frac{2s_a+1}{2s_b+1}\frac{NRS}{2s+1}\sigma_{\mathrm{JULIE}}(\theta),$$

where s_b and s_a are the spins of the incoming and outgoing particles, respectively, s is the spin of the transferred nucleon, S is the spectroscopic factor, and NR accounts for the overlap of the α particle and the n-^{3}He system as well as the strength of the interaction. The quantity NR is usually regarded as an empirical parameter determined by comparison with results of (d,p) or (p,d) reactions or from sum-rule requirements. The value $NR=(6.53)(14.1)=92.1$ obtained[2] from the comparison of ^{92}Zr(^{3}He,α) and ^{92}Zr(p,d) was used in the present work. This value is in excellent agreement with the value of $92.0\pm 20\%$ obtained from an extensive analysis of (^{3}He,α) reactions at 18-MeV bombarding energy.[20] It may be mentioned that Bassel[21] has successfully calculated the normalization factor required for (^{3}He,d) reactions by using a realistic wave function for the ^{3}He ion. Extending the same type of calculation to

[14] H. W. Broek, J. L. Yntema, B. Buck, and G. R. Satchler, Nucl. Phys. **64**, 259 (1965).
[15] S. F. Eccles, H. F. Lutz, and V. A. Madsen, Phys. Rev. **141**, 1067 (1966).
[16] G. R. Satchler, Nucl. Phys. **70**, 177 (1965).
[17] E. F. Gibson, J. J. Kraushaar, B. W. Ridley, M. E. Rickey, and R. H. Bassel, Phys. Rev. **155**, 1208 (1967).
[18] P. H. Stelson and F. K. McGowan, Nucl. Phys. **32**, 652 (1962).
[19] P. Darriulat, G. Igo, H. G. Pugh, J. M. Meriwether, and S. Yamabe, Phys. Rev. **134**, B42 (1964).
[20] R. Stock, R. Bock, P. David, H. H. Duhm, and T. Tamura, Nucl. Phys. **A104**, 136 (1967).
[21] R. H. Bassel, Phys. Rev. **149**, 791 (1966).

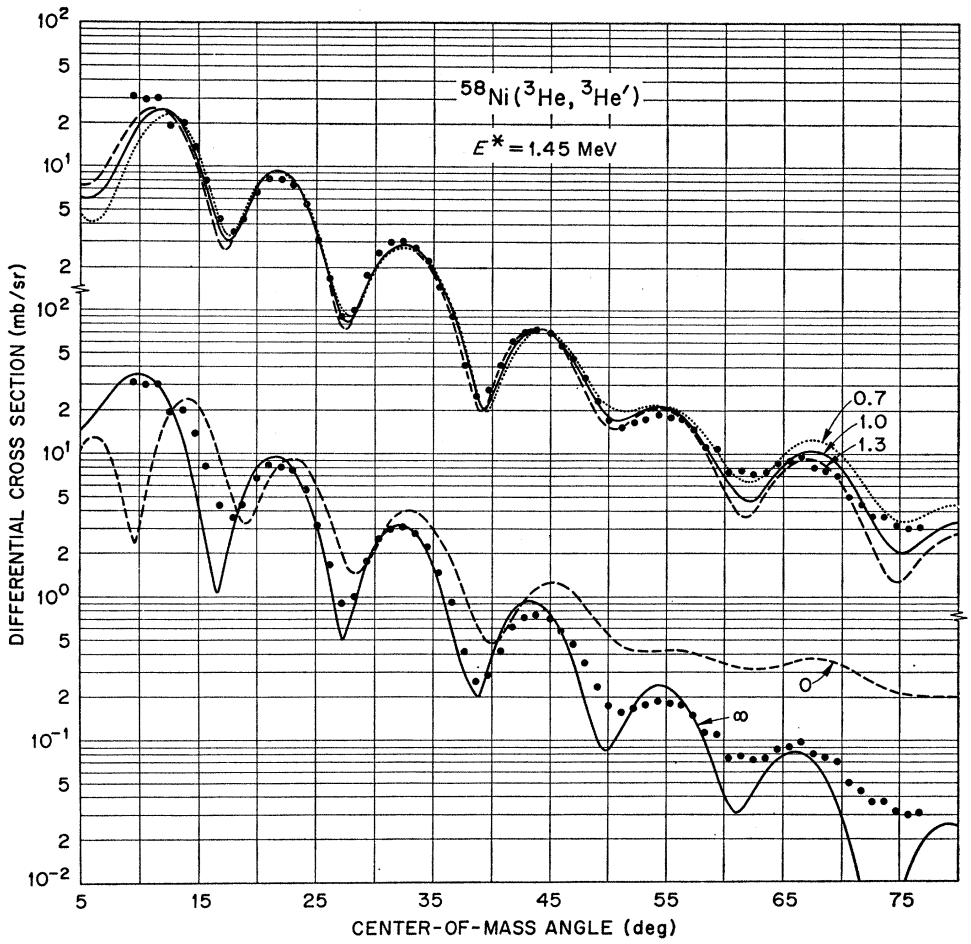

FIG. 6. Comparison of distorted-wave predictions with the experimental data for the first 2^+ state. The experimental data, represented by the points, are the same in both parts. The ratio β_I/β_R is given for each curve.

TABLE III. Results from ^{58}Ni(^{3}He,^{3}He′), using potential *C*, in comparison with other experimental results.

		Present results			Other results		
E^*(MeV)	l	β	βR_0	$\beta R_0'$	β	βR_0	$\beta R_0'$
1.45	2	0.163	0.625	1.045	0.24[a], 0.16[b], 0.17[c], 0.15[d], 0.214[e]	1.16[a], 1.01[b], 1.05[c], 0.93[e]	1.05[b], 0.90[d]
4.44	3	0.138	0.529	0.884	0.19[a], 0.14[b], 0.18[c], 0.12[d]	0.92[a], 0.88[b], 1.11[c]	0.92[b], 0.75[d]
6.75	3	0.078	0.299	0.500			
7.13	3	0.075	0.288	0.481			

[a] Inelastic scattering of protons at 19 MeV (Ref. 15).
[b] Inelastic scattering of α particles at 43 MeV (Ref. 14).
[c] Inelastic scattering of α particles at 28 MeV (Ref. 16).
[d] Inelastic scattering of ^{4}He particles at 37.7 MeV (Ref. 17).
[e] Coulomb excitation [Ref. 18 (quoted in Ref. 14 with correction for rounded charge distribution)].

TABLE IV. Parameters from least-squares fitting of angular distributions from Ref. 19 for elastic scattering of 64.3-MeV α particles by ^{58}Ni.

Potential	V_0 (MeV)	W_0 (MeV)	r_0 (F)	a (F)	σ_R (mb)
J	105.15	37.56	1.404	0.621	1599
K	150.0	49.95	1.350	0.618	1594

(^{3}He,α) reactions, he predicts[22] a value of $NR \simeq 76$. This is only 18% lower than the empirical result quoted above.

[22] R. H. Bassel (private communication).

The distorted-wave predictions are compared with the experimental angular distributions in Fig. 4. The spectroscopic factors are given in Table V. Spin assignments made previously[4–7] were entirely consistent with the present data. However, because of the somewhat featureless angular distributions for the higher l transfers, it is difficult to make assignments on the basis of the angular distribution alone, as illustrated for the 5.91-MeV angular distribution in Fig. 4.

The spectroscopic factors are compared with the (p,d) results at 18.5 MeV,[6] and the (^{3}He,α) results at 15 MeV,[5] 18 MeV,[5] and 25 MeV [4] in Table V. In general

TABLE V. Properties of ^{57}Ni levels from single-neutron pickup reactions on ^{58}Ni.

(^{3}He,α) at 51 MeV[a]			(p,d) at 18.5 MeV[b]			(^{3}He,α) at 25 MeV[c]			(^{3}He,α) at 15 and 18 MeV[d]			
Excitation energy E^* (MeV)	l_j	S	E^*	l	S	E^*	l_j	S	E^*	l_j	S 15 MeV	S 18 MeV
0.0	$p_{3/2}$	1.00	0.0	1	0.90	0.0	$p_{3/2}$	1.08	0.0	$p_{3/2}$	1.06	1.10
0.76	$f_{5/2}$	0.79	0.74	3, 1	0.60, 0.08	0.76	$f_{5/2}$	0.86	0.75	$f_{5/2}$	0.71	0.69
1.10	$p_{1/2}$	0.29	1.04	1	0.10	1.08	$p_{1/2}$	0.13	1.05	$p_{1/2}$	0.23	0.21
2.55	$f_{7/2}$	2.78	2.46	3	2.0	2.58	$f_{7/2}$	2.59	2.55	$f_{7/2}$	2.71	2.88
3.22	$f_{7/2}$	0.68				3.26	$f_{7/2}$	0.69	3.25	$f_{7/2}$	1.01	0.81
3.69	$f_{7/2}$	0.30				3.83	$f_{7/2}$	0.43				
4.20	$f_{7/2}$	0.34				4.26	$f_{7/2}$	0.37				
4.54	$f_{7/2}$	0.41				4.59	$f_{7/2}$	0.45				
5.22	$f_{7/2}$	2.39				5.28	$f_{7/2}$	2.41	5.25	$f_{7/2}$	3.22	3.12
									5.57	$f_{7/2}$	1.27	1.38
5.91	$f_{7/2}$	0.58				6.12	$f_{7/2}$	0.91	6.05	$f_{7/2}$	0.85	1.00
Sum	$p+f_{5/2}$	2.08										
Sum	$f_{7/2}$	7.48										

[a] Present results. [b] Reference 6. [c] Reference 4. [d] Reference 5.

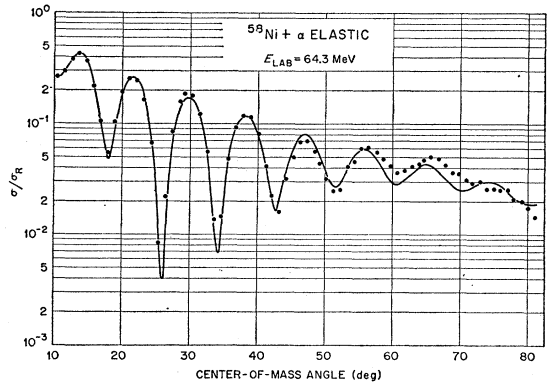

FIG. 7. Ratio of elastic scattering cross section to the Rutherford cross section for 64.3-MeV α particles on ^{58}Ni (from Ref. 19). The curve is the fit with potential J of Table IV.

the agreement is quite good. Many of the spectra show a peak near 5.5 MeV (see, for example, Fig. 1). If this group is identified as the $f_{7/2}$ state at 5.57 MeV of Ref. 5, its spectroscopic factor would be $\approx$0.5. However, the peak shifted and changed intensity with angle with respect to the neighboring $f_{7/2}$ peaks, which suggests that the 5.5-MeV group is not exclusively $f_{7/2}$. It appears that other states in this region are also populated, and their angular distributions oscillate more rapidly than expected for an $f_{7/2}$ transition.

Good agreement with theoretically expected values was obtained. The $f_{7/2}$ state at 5.22 MeV is the isobaric analog of the ^{57}Co ground state.[7] From the formula developed by French and Macfarlane,[23] one expects a spectroscopic factor of 2.67, in agreement with the present result. The calculation for the analog state used the usual separation-energy prescription. No attempt was made to do a coupled-channel calculation as discussed in Ref. 20. The isotopic spin of the target ground state is 1, so the inaccuracy introduced by using the separation-energy procedure is not expected to be large. The sum of the $f_{7/2}$ spectroscopic factors is theoretically expected to be 8.0, and the sum of the spectroscopic factors for $f_{5/2}$ and p states is expected to be 2.0. The present results agree well with both sum-rule predictions.

ACKNOWLEDGMENTS

We wish to thank A. H. Funaro for his help in the analysis of the data, and R. H. Bassel and R. M. Drisko for many enlightening discussions. The support of R. S. Livingston and A. Zucker is gratefully acknowledged.

[23] J. B. French and M. H. Macfarlane, Nucl. Phys. 26, 161 (1961).